# Core-level and valence-band study using angle-integrated photoemission on LaFeAsO$_{0.9}$F$_{0.1}$

D. R. Garcia,[1,2] C. Jozwiak,[1] C. G. Hwang,[2] A. Fedorov,[3] S. M. Hanrahan,[4] S. D. Wilson,[2] C. R. Rotundu,[2]
B. K. Freelon,[2] R. J. Birgeneau,[1,2] E. Bourret-Courchesne,[2] and A. Lanzara[1,2,*]

[1]*Department of Physics, University of California—Berkeley, Berkeley, California 94720, USA*
[2]*Materials Sciences Division, Lawrence Berkeley National Laboratory, Berkeley, California 94720, USA*
[3]*Advanced Light Source, Lawrence Berkeley National Laboratory, Berkeley, California 94720, USA*
[4]*Life Sciences Division, Lawrence Berkeley National Laboratory, Berkeley, California 94720, USA*

Using angle-integrated photoemission spectroscopy we have probed the novel LaFeAsO$_{0.9}$F$_{0.1}$ superconductor over a wide range of photon energies and temperatures. We have provided a full characterization of the orbital character of the valence-band (VB) density of states (DOS) and of the magnitude of the $d$-$p$ hybridization energy. Finally, we have identified two characteristic temperatures: 90 K where a pseudogap-like feature appears to close and 120 K where a sudden change in the DOS near $E_F$ occurs. We associate these phenomena with the spin density wave magnetic ordering and the structural transition seen in the parent compound, respectively. These results suggest the important role of electron correlation, spin physics, and structural distortion in the physics of Fe-based superconductors.

## I. INTRODUCTION

With the recent discovery of remarkably high temperature superconductivity in the fluorine doped LaFeAsO$_{1-x}$F$_x$ (Ref. 1), there has been an enormous effort to understand these materials in order to discover whether the nature of their superconductivity is similar to that seen in the well-known high-temperature superconducting (SC) cuprates or if it is of a completely different type altogether. One reason for the potential uniqueness of these compounds is that bands related to Fe appear to dominate the near $E_F$ band structure and are hence responsible for superconductivity.[2] This is unlike the superconducting cuprates where superconductivity is believed to occur in the CuO plane and, thus, could open the door for additional magnetic degrees of freedom in the FeAs systems. This situation, together with the proposed strong hybridization between the Fe 3$d$ and As 4$p$ orbitals needed to explain the anomalously small value of the Fe magnetic moment,[3] begins to place the Fe-based superconductors in a strong correlation regime as is already the case for the cuprate superconductors. Additionally, the LaFeAsO parent compound has been observed to have both an antiferromagnetic spin density wave (SDW) phenomenon at ∼134 K, along with a structural distortion at ∼150 K.[4,5] This latter phenomenon is believed to be an important parameter for modulating both the $d$-$p$ hybridization and the onset of the antiferromagnetic fluctuation.[3] The presence of these phenomena in the LaFeAsO$_{1-x}$F$_x$ phase diagram and their apparent competition with the superconducting phase further underscore the complex physics of these materials and their near $E_F$ properties.[4,6,7]

Despite the numerous angle-integrated and angle-resolved photoemission results that have appeared in the literature in the past few months,[8–15] basic knowledge of the electronic structure of these materials, the importance of the correlation effects, and how the spin physics modulates the near $E_F$ states are still not fully understood. So far, limited data on the orbital nature valence-band (VB) spectra exists and no

measurements of the proposed strong $p$-$d$ hybridization are available. Similarly no current understanding of the role of the structural distortion[4,5] on the near $E_F$ states exist. These concerns, along with the current controversy over the role of spin fluctuations[2,4,6,7,16–22] in explaining the low energy features of the near $E_F$ density of states (DOS), are certainly among the fundamental aspects of these materials that must be addressed before we can come to a complete understanding of the physics of these materials.

In this paper, we use angle-integrated photoemission spectroscopy (AIPES) on polycrystalline LaFeAsO$_{0.9}$F$_{0.1}$ ($T$ =25 K) to address these issues. We explore the origins of core-level peaks, the valence-band density of states (VB DOS), and near $E_F$ features over a range of photon energy and temperature. We identify all expected core levels within our energy range and provide an experimental characterization of the orbital character of the VB DOS. We find an anomalously large splitting (0.65 eV) of the As 3$d$ orbital as well as an unexplained satellite feature associated with it, which allow us to provide bounds on the magnitude of the Fe/As hybridization that are consistent with recent theoretical work, to explain the origin of the anomalously low Fe 3$d$ magnetic moment.[3] Finally, we report significant changes in the near $E_F$ spectra at two characteristic temperatures, 90 and 120 K, which we identify with the closing of a pseudogap-like feature and the onset of a structural transition, respectively. This work suggests that strong correlations related to spin physics, such as the phenomena observed in the undoped parent compound, need to be included in our understanding of the superconducting state in these FeAs systems.

## II. EXPERIMENTAL PROCEDURE

Samples of polycrystalline LaFeAsO$_{0.9}$F$_{0.1}$ were synthesized by solid state reactions. La and As metals were mixed and reacted in an evacuated sealed quartz ampoule at 500 °C for 12 h, followed by a reaction at 850 °C for 2 h. The formation of LaAs was confirmed by x-ray diffraction.
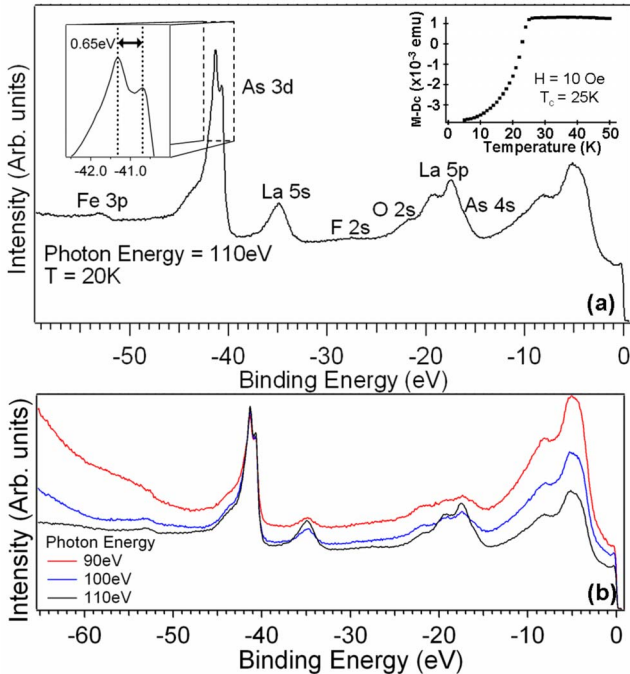
FIG. 1. (Color online) (a) Core-level spectroscopy of LaFeAsO$_{0.9}$F$_{0.1}$ taken in the SC phase using 110 eV photon energy. The upper right inset shows the measured $T_c$ of our sample. (b) Core-level spectrum from (a) taken at three different photon energies. The spectra are normalized to photon flux and show differing trends in intensity based on orbital character.

Fe$_2$O$_3$, Fe, and LaF$_3$ were then mixed with LaAs and loaded into a tantalum tube. The amount of LaF$_3$ was calculated to provide 10% F. The tube was crimped and sealed in an evacuated quartz ampoule. The reaction was carried out at 1150 °C for 50 h. The final product: LaAsFeOF was confirmed by x-ray diffraction. The sample has a critical temperature of 25 K as determined by the diamagnetic transition in our magnetization measurements, shown in the inset of Fig. 1.[23] Synchrotron photoemission spectroscopy data were taken at Beamline 12.0.1 at the Advanced Light Source of the Lawrence Berkeley National Laboratory using a Scienta SES100 hemispherical analyzer and also at Beamline 5.4 at the Stanford Synchrotron Radiation Laboratory, using a Scienta R4000 analyzer. The energy resolution was 0.1 eV for both the core-level and VB data. A resolution of 25 meV was used for the near $E_F$ data in Fig. 3, while 5 meV was achieved for the data presented in Fig. 4. Sample surfaces were prepared both by cleaving the polycrystalline rod *in situ*, and by a cleaving followed with gentle scraping *in situ* of the exposed surface using a diamond file. Both were done at a temperature less than 25 K and a base pressure better than $5 \times 10^{-11}$ torr. From our experiments and the data presented, we found no quantitative differences between these two methods.

## III. RESULTS

### A. Core-level spectra

Figure 1 shows core-level spectra taken in the superconducting phase along with the atomic orbitals associated with

them. Within the energy window of Fig. 1, we identify the expected La core levels: La 5$s$ at 35.0 eV, La 5$p_{1/2}$ at 19.0 eV, and La 5$p_{3/2}$ at 17.5 eV. Similarly, the only expected oxygen core level in this energy window is the O 2$s$ peak, which is generally expected near 20 eV in other oxides[24] and thus we identify it with the shoulder to the left of the mentioned La 5$p$ orbitals. A greater difficulty comes with resolving the fluorine core level peaks. It is expected that the F 2$p$ binding energy should be only a few eV larger than the O 2$p$ orbital.[24] As theory suggests and we will argue in Sec. III B, the spectral weight between 5 and 10 eV is dominated by the O 2$p$ orbital, putting the likely weaker F 2$p$ orbital contribution underneath this spectra. Nevertheless, we interpret the weak, broad feature at 27 eV as the F 2$s$ orbital expected at a roughly 20 eV higher binding energy than F 2$p$. As for the Fe core level, we can successfully resolve the Fe 3$p$ orbital, although we are unable to resolve any potential splitting between the 3$p_{1/2}$ and 3$p_{3/2}$, most likely due to the weak intensity. Surprisingly, when we look at the As 3$d$ core level, we observe a splitting between the 3$d_{3/2}$ (40.7 eV) and 3$d_{5/2}$ (41.3 eV) peaks of ~0.65 eV, which is much larger than what was observed for As in its natural form[25] and is ~.05 eV (Ref. 26) larger than observed in the undoped parent compound LaFeAsO. Within our resolution, the magnitude of such splitting is temperature independent, above and below $T_c$. This large splitting suggests that we are in a regime where the hybridization between the Fe 3$d$ and the As 4$p$ orbitals is quite strong as previously proposed.[3,27] Modeling the splitting as due to hybridization between Fe 3$p_{3/2}$ and the As 3$d_{3/2}$ orbitals with a two-level model,[28] we can put experimental constraints on the magnitude of the Fe/As hybridization energy, finding it to be between 1.1 and 1.4 eV. This is consistent with the values required to explain the anomalously small Fe magnetic moment reported for these materials.[3]

Finally, we did resolve two additional features in the core-level study which do not directly correspond to any known orbital core level: (a) a subtle shoulder at ~16 eV near the La 5$p$ peaks and (b) a well-defined shoulder at ~44 eV, to the left of the As 3$d$ peak. Because their binding energies are photon energy independent, neither of these features can be associated with a secondary peak or an Auger peak. For the former feature, one possibility is to associate it with the currently unresolved As 4$s$ peak, although shifted by ~4 eV from its expected value. A second possibility is to consider it a satellite feature associated with the La 5$p$ orbitals. Photon energy dependence, as explained later on, leads us to the first conclusion, associating the feature with the weaker As 4$s$ state, yet the reason for the apparent energy shift in this peak remains unclear.

For the latter feature, the absence of any expected additional peak within the energy range leads us to suspect it to be a satellite feature of the As 3$d$ peaks related to the critical FeAs layer, particularly to the Fe 3$p$-As 3$d$ strong hybridization previously proposed to explain the observed As 3$d$ splitting. This feature appears to be unchanged above and below $T_c$. Modeling the spectra near the As 3$d$ peaks with multiple Lorentzian peaks, we estimate the peak in this satellite feature to appear around ~43 eV, a separation of more than 1.5 eV from the As 3$d_{3/2}$ peak. Satellite structures in fact arise

from Coulombic attraction between a core hole created by photoemission and the VB states and have been instrumental in the study of other materials: the Cu $2p$ orbital in high $T_c$ cuprates[29] and the Ru $3d$ orbital in the ruthenates.[30] One possibility is that the considerable As $4p$ character that theory expects around 1.5 eV above $E_F$ (Refs. 2, 27, 31, and 32) could cause a satellite peak to form around 2–3 eV from the As $3d$ peaks as these As $3d$ core electrons are photoemitted, potentially explaining the observed shoulder.

To further confirm our analysis, we have performed a detailed photon energy dependent study of the entire core-level region. Photon energy dependent photoemission has the advantage that the photoemission cross section changes uniquely for different elements. Core-level spectra at a few characteristic photon energies are shown in Fig. 1(b). A clear enhancement of the peaks near 35, 19, and 18 eV, already identified with the La $5s$ and the $5p$ orbitals, is observed when the photon energy approaches the La $4d$ core-level resonance (at ~105 eV). This supports the La nature of these peaks and gives weight to the prior hypothesis that the additional energy shoulder near 16 eV, which is not similarly enhanced but appears relatively stronger in the 90 eV curve, is indeed unrelated to La and is of an As $4s$ origin.

### B. Valence-band spectra

Having identified all the core-level peaks in the spectra, the next crucial step is to identify the nature of the valence-band region below 15 eV. Although much theoretical work has proposed that this region is mostly dominated by oxygen and iron contributions,[2,27,31,32] so far there has not been a complete experimental characterization of this region. Photon energy dependent photoemission can provide direct information on the DOS since, as mentioned, the photoemission cross section changes uniquely for different elements. In order to better discern the relative O and Fe concentrations, Fig. 2(a) focuses on the VB region between $E_F$ and 25 eV in binding energy. The spectra are renormalized to the peak near 5 eV, which allows one to distinguish the 3–15 eV VB region from the sharp feature seen at ~0.3 eV. Since the photoemission cross section is known to decrease faster for O than Fe over this photon energy range,[33] seeing the increase in the 0.3 eV feature relative to the remaining VB region helps confirm its orbital character as Fe $3d$ while the remaining VB has a majority O $2p$ character, a fact also hinted to by prior DOS calculations.[2,31,32] We also note that although we clearly observe this Fe $3d$ peak at nearly 0.3 eV when using higher photon energies (50–110 eV), the peak does appear to be shifted closer to 0.2 eV when we employ a lower photon energy (23 eV). This is not surprising since the peak is quite likely composed of multiple bands which may also be relatively enhanced with different photon energies.

To explore additional orbital character within the VB, Fig. 2(b) compares spectra taken with both 100 and 50 eV light. Although the proposed La $5p$ and Fe $3d$ peaks only change in relative peak intensity, the remaining VB is greatly affected, particularly near 10 eV with new peak features being enhanced. The proximity of the 50 eV data to the Fe $3p$ resonance at 53 eV leads us to focus on two points. First, the
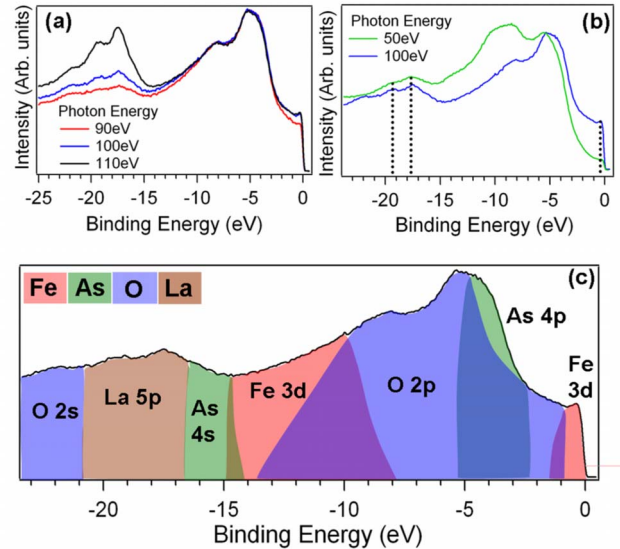


FIG. 2. (Color online) (a) The VB region from Fig. 1(b) now normalized to the peak near 5 eV binding energy. This helps distinguish Fe from O orbitals in the VB. (b) VB spectra taken with 50 and 100 eV photon energy. The dashed lines mark the locations of the La $5p$ and Fe $3d$ peaks. (c) A cartoon summarizing our proposed assignments of orbital character to different regions of the VB DOS based on the data from (a) and (b) and Fig. 1.

sudden appearance of a feature near 13 eV in the 50 eV data suggests an Fe orbital character to this region within the VB. Indeed, a closer examination of that energy region (10–14 eV) in Fig. 2(a) shows that the spectral intensity actually does increase similarly to the increase seen in the 0.3 eV feature already attributed to Fe $3d$. Thus, one can speculate that this region of the VB DOS has a larger Fe $3d$ contribution than at slightly lower binding energy. That would explain the origin of the additional peak structure at ~10 eV appearing in the 50 eV data when compared to the higher photon energy data. Second, in light of this analysis, we can also attempt to make some sense of the strong ~5 eV feature in the DOS. A close examination of the feature at higher photon energy clearly shows that at least two peaks are likely responsible for the slightly asymmetric line shape. The change in line shape between the 100 and 50 eV data leads us to suspect that an additional nonoxygen orbital may be contributing to the overall spectral weight. From our analysis of Fig. 1(b), La seems unlikely. Furthermore, the bandwidth change between 100 and 50 eV of this feature appears to become narrower, suggesting the additional spectral weight is weakened at 50 eV, making Fe $3d$ unlikely. In light of these observations, we propose that although the primary character of this peak appears to be O $2p$, the additional spectral weight at lower binding energy is related to As, most likely the previously unaccounted for $4p$ orbital whose hybridization with Fe $3d$ was discussed earlier. Figure 2(c) provides a cartoon to qualitatively summarize our conclusions regarding the orbital character of the VB DOS.

### C. Near-$E_F$ spectra

We now turn our attention from the VB to the near $E_F$ spectra and its evolution with photon energy and tempera-
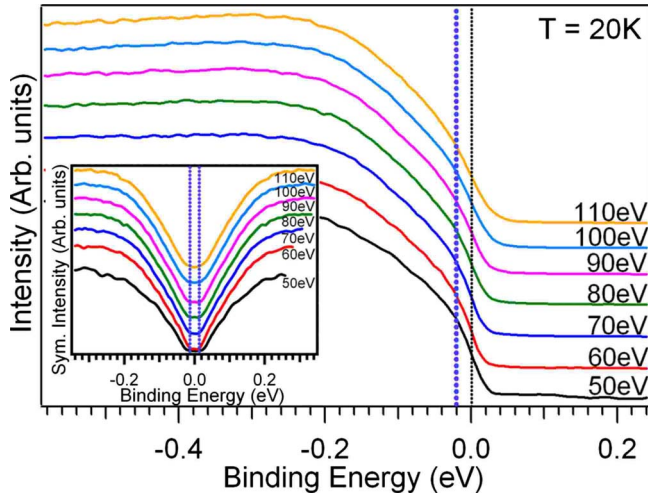
FIG. 3. (Color online) Near $E_F$ data taken over a range of photon energies from 50 to 110 eV at $T=20$ K. The blue dotted line indicates the energy scale of the spectral feature 15 meV below $E_F$. The inset symmetrizes the data to remove contributions from the Fermi function. The blue dotted lines indicate the $2\Delta \sim 30$ meV gap feature which we see at all energies.

ture. Although AIPES measurements have already been carried out in these materials[8–10,12] and recent ARPES works focusing on the near $E_F$ region of related FeAs systems are now becoming available,[13–15] the current studies are lacking a detailed temperature dependence analysis, thus leading to controversy on the origin of the different energy scales identified.[9–12] With AIPES being able to directly measure the DOS as we have done for the VB region, we can focus near $E_F$ to discern gap and pseudogap features in the spectra.[34]

Figure 3 shows the photon energy dependence of the near $E_F$ spectra. As previously reported,[9,10] the spectra show a sharp discontinuity near the Fermi level which is robust over photon energy. This discontinuity can be better visualized by symmetrizing the data about $E_F$ to remove the contribution from the Fermi function (inset of Fig. 3). For clarity, it is worth noting that although the symmetrization technique could appear to suggest zero spectral intensity at $E_F$, this is not the case as the main Fig. 3 clearly shows. With the symmetrized data, the discontinuity is manifested by a plateau region, with a width of 30 meV (indicated by the blue dotted lines in the inset), which likely represents the previously reported 15 meV gap.[10,12] From our photon energy dependent study, we observe an enhancement of this feature when 50 eV photons are used. This is in agreement with the Fe $3d$ nature of the near $E_F$ bands, as previously discussed, and is likely due to the vicinity of the photon energy to the Fe $3p$ resonance at 53 eV. Finally, we note that, given the energy resolution of these data, we do not expect to cleanly resolve the small superconducting gap ($\Delta \sim 4$ meV at 5 K).[10]

To shed light on the current debate on the origin of the 15 meV gaplike feature,[9–12] Fig. 4 shows its temperature dependence by performing a high resolution study on the near $E_F$ spectra. The 15 meV feature is indicated by the dotted blue arrow in Fig. 4(a). Some indications of its temperature dependence are already obvious in the raw data and in the gradual disappearance of the feature near 15 meV in the first derivative spectra [Fig. 4(b)]. To gain more detailed information on the temperature evolution of this feature, we show symmetrized spectra of Fig. 4(a) to once again remove any thermal broadening contribution arising from the Fermi function. The data show an interesting evolution with temperature, which leads us to identify the following two character-
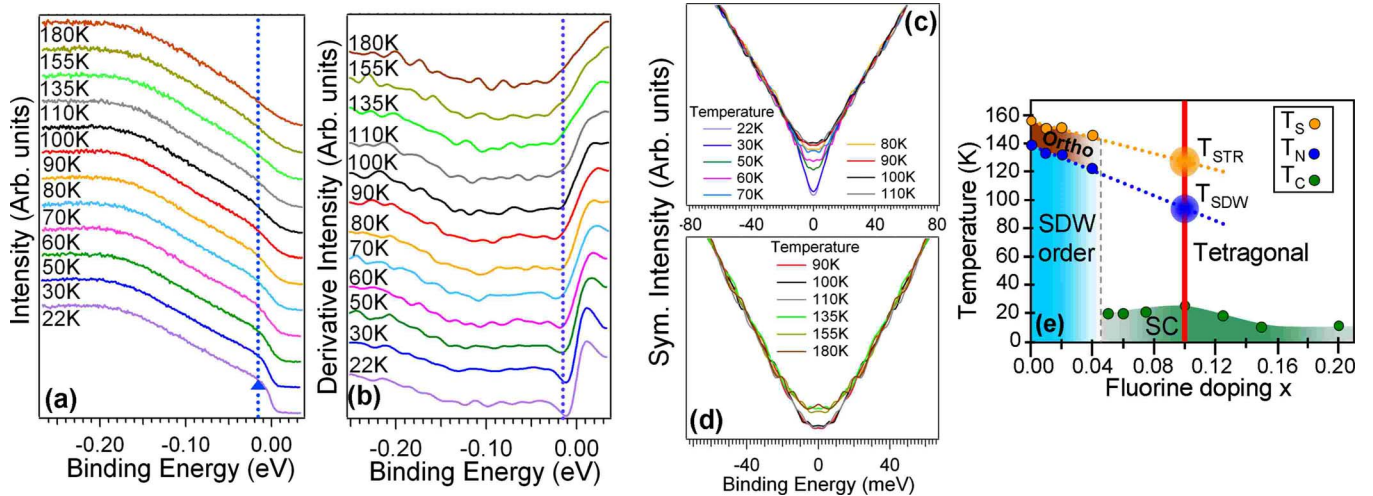


FIG. 4. (Color online) (a) Higher resolution temperature dependent data taken with 23 eV photon energy. The blue dotted line with arrow indicates the near $E_F$ features noted in Fig. 3 at 15 meV. (b) First derivative taken of the data from (a) symmetrized. The temperature dependent dip near $E_F$ corresponds to the 15 meV feature and this energy scale is, again, marked by the blue dotted line. (c)–(d) Symmetrized data from (a) near $E_F$. In (c), we see the gradual temperature evolution of the 15 meV pseudogap feature until the evolution stops around 90 K. In (d), the temperature increase continues with a second abrupt change in the near $E_F$ DOS line shape between 110 and 135 K. (e) Using phase diagram data from Ref. 35, we take the $T_N$ temperatures (blue dots) which define the SDW phase and extrapolate them (blue line) to determine the potential transition temperature for the SDW phase at doping $x=0.1$ (red line), finding a $T_{SDW} \sim 90$ K, associating this with (c). This is similarly done for the orthorhombic-tetragonal structure transition temperatures, $T_S$ (yellow dots), to find the potential transition temperature at $x=0.1$, $T_{str} \sim 120$ K, associating this with (d).

istic temperatures: (1) $T=90$ K, which is the temperature where the gaplike feature "closes up" after a gradual evolution in the line shape with increasing temperature as suggested by the first derivative data [Fig. 4(b)] and further indicated by the symmetrized data shown in Fig. 4(c) and (2) a temperature between 110 and 135 K where an abrupt change in the shape of the DOS is observed [shown in Fig. 4(d)], and then remains unchanged for all increasing temperatures, up to at least 180 K.

## IV. DISCUSSION

To understand the nature of these two temperatures, we examine the known phase diagram for the LaFeAsO$_{1-x}$F$_x$ system shown in Fig. 4(e).[35] As discussed in Sec. I, the undoped parent compound contains both a magnetic ordering and a structural transition above 100 K. Whether such ordering is suppressed by the fluorine doping is still controversial as several experimental results seem to suggest its persistence all the way to $x=0.1$ doping.[17–22] Comparing the extrapolated temperatures for the structural ($T_{str}$) and SDW transitions ($T_{SDW}$), there is a good agreement between these two temperatures and the two temperatures identified in our data where the DOS undergoes a change. This leads us to speculate that, although the electron doping of the parent compound clearly competes with the magnetic ordering and structural transition, the coexistence of these phases at higher doping, where superconductivity exists, is in fact occurring and responsible for the observed features. Thus, we interpret the 15 meV feature as a pseudogap-like feature related to the SDW magnetic ordering, which closes around $T_{SDW}=90$ K, and we interpret the subtler effect in the DOS around $T_{str}$ $=120$ K as the structural transition seen in the parent compound.

## V. CONCLUSION

In conclusion, we have used photon energy and temperature dependent angle-integrated photoemission spectroscopy to explore core-level peaks, the VB DOS, and near $E_F$ features in polycrystalline LaFeAsO$_{0.9}$F$_{0.1}$. We have identified the nature of all the core-level peaks and features, and we have provided evidence detailing the orbital character of the VB DOS. We have found an anomalously large splitting of the As $3d$ peak and have explained it as a consequence of the anomalously low Fe magnetic moment. Finally, we have identified two characteristic temperatures: 90 K where a pseudogap-like feature closes up and 120 K where a more sudden change in the DOS occurs. We associate these with the SDW magnetic ordering and structural transition temperatures, respectively. This result suggests that the electron doped superconducting phase does not entirely suppress the magnetic phenomena in the FeAs plane as some recent theory has suggested.[36]

*alanzara@lbl.gov

[1] Y. Kamihara, T. Watanabe, M. Hirano, and H. Hosono, J. Am. Chem. Soc. **130**, 3296 (2008).

[2] Fengjie Ma and Zhong-Yi Lu, Phys. Rev. B **78**, 033111 (2008).

[3] J. Wu, P. Phillips, and A. H. Castro Neto, Phys. Rev. Lett. **101**, 126401 (2008).

[4] C. de la Cruz, Q. Huang, J. W. Lynn, Jiying Li, W. Ratcliff II, J. L. Zarestky, H. A. Mook, G. F. Chen, J. L. Luo, N. L. Wang, and Pengcheng Dai, Nature (London) **453**, 899 (2008).

[5] H. H. Klauss, H. Luetkens, R. Klingeler, C. Hess, F. J. Litterst, M. Kraken, M. M. Korshunov, I. Eremin, S. L. Drechsler, R. Khasanov, A. Amato, J. Hamann-Borrero, N. Leps, A. Kondrat, G. Behr, J. Werner, and B. Büchner, Phys. Rev. Lett. **101**, 077005 (2008).

[6] J. Dong, H. J. Zhang, G. Xu, Z. Li, G. Li, W. Z. Hu, D. Wu, G. F. Chen, X. Dai, J. L. Luo, Z. Fang, and N. L. Wang, Europhys. Lett. **83**, 27006 (2008).

[7] S. Kitao, Y. Kobayashi, S. Higashitaniguchi, M. Saito, Y. Kamihara, M. Hirano, T. Mitsui, H. Hosono, and M. Seto, J. Phys. Soc. Jpn. **77**, 103706 (2008).

[8] H. W. Ou, J. F. Zhao, Y. Zhang, D. W. Shen, B. Zhou, L. X. Yang, C. He, F. Chen, M. Xu, T. Wu, X. H. Chen, Y. Chen, and D. L. Feng, Chin. Phys. Lett. **25**, 2225 (2008).

[9] Y. Ishida, T. Shimojima, K. Ishizaka, T. Kiss, M. Okawa, T. Togashi, S. Watanabe, X.-Y. Wang, C.-T. Chen, Y. Kamihara, M. Hirano, H. Hosono, and S. Shin, arXiv:0805.2647 (unpublished).

[10] T. Sato, S. Souma, K. Nakayama, K. Terashima, K. Sugawara, T. Takahashi, Y. Kamihara, M. Hirano, and H. Hosono, J. Phys. Soc. Jpn. **77**, 063708 (2008).

[11] Haiyun Liu, Xiaowen Jia, Wentao Zhang, Lin Zhao, Jianqiao Meng, Guodong Liu, Xiaoli Dong, G. Wu, R. H. Liu, X. H. Chen, Z. A. Ren, Wei Yi, G. C. Che, G. F. Chen, N. L. Wang, Guiling Wang, Yong Zhou, Yong Zhu, Xiaoyang Wang, Zhongxian Zhao, Zuyan Xu, Chuangtian Chen, and X. J. Zhou, Chin. Phys. Lett. **25**, 3761 (2008).

[12] Xiaowen Jia, Haiyun Liu, Wentao Zhang, Lin Zhao, Jianqiao Meng, Guodong Liu, Xiaoli Dong, G. F. Chen, J. L. Luo, N. L. Wang, Z. A. Ren, Wei Yi, Jie Yang, Wei Lu, G. C. Che, G. Wu, R. H. Liu, X. H. Chen, Guiling Wang, Yong Zhou, Yong Zhu,

Xiaoyang Wang, Zhongxian Zhao, Zuyan Xu, Chuangtian Chen, and X. J. Zhou, Chin. Phys. Lett. **25**, 3765 (2008).

[13] C. Liu, T. Kondo, M. E. Tillman, R. Gordon, G. D. Samolyuk, Y. Lee, C. Martin, J. L. McChesney, S. Bud'ko, M. A. Tanatar, E. Rotenberg, P. C. Canfield, R. Prozorov, B. N. Harmon, and A. Kaminski, arXiv:0806.2147 (unpublished).

[14] C. Liu, G. D. Samolyuk, Y. Lee, N. Ni, T. Kondo, A. F. Santander-Syro, S. L. Bud'ko, J. L. McChesney, E. Rotenberg, T. Valla, A. V. Fedorov, P. C. Canfield, B. N. Harmon, and A. Kaminski, Phys. Rev. Lett. **101**, 177005 (2008).

[15] Lin Zhao, Haiyun Liu, Wentao Zhang, Jianqiao Meng, Xiaowen Jia, Guodong Liu, Xiaoli Dong, G. F. Chen, J. L. Luo, N. L. Wang, Guiling Wang, Yong Zhou, Yong Zhu, Xiaoyang Wang, Zhongxian Zhao, Zuyan Xu, Chuangtian Chen, and X. J. Zhou, Chin. Phys. Lett. **25**, 4402 (2008).

[16] I. I. Mazin, D. J. Singh, M. D. Johannes, and M. H. Du, Phys. Rev. Lett. **101**, 057003 (2008).

[17] Israel Nowik, Israel Felner, V. P. S. Awana, Arpita Vajpayee, and H. Kishana, J. Phys.: Condens. Matter **20**, 292201 (2008).

[18] Israel Felner, Israel Nowik, M. I. Tsindlekht, Zhi-An Ren, Xiao-Li Shen, Guang-Can Che, and Zhong-Xian Zhao, arXiv:0805.2794 (unpublished).

[19] K. Ahilan, F. L. Ning, T. Imai, A. S. Sefat, R. Jin, M. A. McGuire, B. C. Sales, and D. Mandrus, Phys. Rev. B **78**, 100501(R) (2008).

[20] Z. W. Zhu, Z. A. Xu, X. Lin, G. H. Cao, C. M. Feng, G. F. Chen, Z. Li, J. L. Luo, and N. L. Wang, New J. Phys. **10**, 063021 (2008).

[21] R. S. Gonnelli, D. Daghero, M. Tortello, G. A. Ummarino, V. A. Stepanov, J. S. Kim, and R. K. Kremer, arXiv:0807.3149 (unpublished).

[22] A. J. Drew, Ch. Niedermayer, P. J. Baker, F. L. Pratt, S. J. Blun-

dell, T. Lancaster, R. H. Liu, G. Wu, X. H. Chen, I. Watanabe, V. K. Malik, A. Dubroka, M. Roessle, K. W. Kim, C. Baines, and C. Bernhard, arXiv:0807.4876 (unpublished).

[23] In spite of these mentioned postsynthesis analyses, it should be noted that the final fluorine concentration was not additionally verified by any chemical analysis of the final product.

[24] G. Sawatzky (private communication).

[25] *Photoemission in Solids I: General Principles*, edited by M. Cardona and L. Ley (Springer-Verlag, Berlin, 1978).

[26] A. Koitzsch, D. Inosov, J. Fink, M. Knupfer, H. Eschrig, S. V. Borisenko, G. Behr, A. Köhler, J. Werner, B. Büchner, R. Follath, and H. A. Dürr, Phys. Rev. B **78**, 180506 (2008).

[27] Chao Cao, P. J. Hirschfeld, and Hai-Ping Cheng, Phys. Rev. B **77**, 220506(R) (2008).

[28] P. Phillips (private communication).

[29] Z.-X. Shen, J. W. Allen, J. J. Yeh, J.-S. Kang, W. Ellis, W. Spicer, I. Lindau, M. B. Maple, Y. D. Dalichaouch, M. S. Torikachvili, J. Z. Sun, and T. H. Geballe, Phys. Rev. B **36**, 8414 (1987).

[30] Hyeong-Do Kim, Han-Jin Noh, K. H. Kim, and S.-J. Oh, Phys. Rev. Lett. **93**, 126404 (2004).

[31] K. Haule, J. H. Shim, and G. Kotliar, Phys. Rev. Lett. **100**, 226402 (2008).

[32] D. J. Singh and M. H. Du, Phys. Rev. Lett. **100**, 237003 (2008).

[33] J.-J. Yeh and I. Lindau, At. Data Nucl. Data Tables **32**, 1 (1985).

[34] M. Hashimoto, T. Yoshida, K. Tanaka, A. Fujimori, M. Okusawa, S. Wakimoto, K. Yamada, T. Kakeshita, H. Eisaki, and S. Uchida, Phys. Rev. B **75**, 140503(R) (2007).

[35] H. Luetkens, H.-H. Klauss, M. Kraken, F. J. Litterst, T. Dellmann, R. Klingeler, C. Hess, R. Khasanov, A. Amato, C. Baines, J. Hamann-Borrero, N. Leps, A. Kondrat, G. Behr, J. Werner, and B. Buechner, arXiv:0806.3533 (unpublished).

[36] I. I. Mazin and M. D. Johannes, arXiv:0807.3737 (unpublished).